MATERIALS RESEARCH INNOVATIONS
https://doi.org/10.1080/14328917.2018.1512736

Taylor & Francis
Taylor & Francis Group

Corrosion of reinforcement in concrete with fly ash and manufactured sand

J. Mahesh[a], K. Nagamani[b] and T. Jarin[c]

[a]Department of Civil Engineering, Udhya School of Engineering, Chennai, India; [b]Department of Civil Engineering, Govt college of engineering, Chennai, India; [c]Jyothi engineering college of Kerala, India

ABSTRACT

This research article reports the comprehensive experimental studies conducted on the identification of corrosion mechanism. The study is made in two different types of samples taken from reinforced concrete containing class–F Fly ash and steel bar with different fine aggregates such as river sand and manufactured sand. It also reports the study under different curing conditions to find out corrosion attack on fly ash concrete structure. Cement placed by means of Fly ash, concrete mixes prepared with 20%, 30%, 40% weight of cement and using16mm diameter steel bar 100mm length with 25 mm clear cover were used as samples. Corrosion process was investigated in embedded steel bar by using Tafel polarization and AC Impedance methods by using ACM Instruments (UK).This study will help in identifying the level of corrosion between the usage of river sand and the manufactured sand.

ARTICLE HISTORY
Received 11 June 2018
Accepted 13 August 2018

KEYWORDS
Concrete; corrosion; curing; fly ash; impedance; polarization

1. Introduction

Corrosion is the process by which a metal or an alloy deteriorates, because of oxidation, a chemical action that creates iron oxides and that flake away from the base [1]. Corrosion of concrete means degradation of concrete such as spots, cracks, spalling that lead to the loss of strength and dimensions of the concrete member due to corrosion of steel reinforcement embedded in concrete [2,3]. The steel reinforcement in fly ash concrete has received an increasing attention in recent years. Because of fly ash availability in cheaper cost, much more quantity is used in construction Industry. Fly ash is a byproduct of the coal fired thermal power plant which has the combination of (Anthracite, Bituminous-class F), (Lignite, sub bituminous–class C).

Fly ash is generally captured by electrostatic precipitators (ESP) before the flue gases reach the chimney which is well accepted as a pozzolonic material used either as a component of ordinary Portland cementor as a mineral admixture in concrete [4]. Fly ash is excellent void filler than Portland cement in concrete . The cost of fly ash is cheaper than OPC. The chemical composition of fly ash consists of 95% to 99% of oxides of silicon, aluminum, calcium in the form of Silicon Oxides (SiO_2), Aluminum Oxides (Al_2O_3), and Calcium Oxides (CaO), Iron Oxides (Fe_2O_3), remaining of trace elements. Carbon content in the fly ash is measured by the Loss on Ignition (LOI). Fly ash occurs as very fine particle having an average diameter less than 10μm with solid and hollow spheres in shape, and have high surface area 300 to 500 sq.m/kg, specific gravity between 1.9 to 2.8, low to medium bulk density 540 to 860 kg/cum without compaction, and 1120 to 1500 kg/cum with compaction and very light texture grey or tan in color.

The quality of fly ash varies depending on the quality of coal which is being used and also depends on the operating condition of the thermal power plant. The main reason for corrosion in fly ash concrete is combination of the mixture of chloride iron (Cl^-)and carbonization [5]. The corrosion of reinforcement in fly ash concrete is the electrochemical process with the presence of oxygen and water [6, 7]. The high alkaline environment (pH>11) protects the steel reinforcement from corrosion. The factors that affect the rate and level of corrosion are pH of the concrete pore water, crack in the concrete, carbonization of cement paste, stray current, design features of concrete, mixture proportions of the concrete, thickness of concrete, concrete cover, and galvanic effect. The concrete deterioration occurs due to rust (Ferric oxides and Ferric hydroxides) formed at the interface between reinforcement and concrete with the rust volume of 3 to 6 times more than Fe iron. Rust creates internal stresses in concrete member [8,9]. Due to Internal stresses cracks will form on the surface of concrete which subsequently damage the concrete structure that finally lead to the collapse of the entire concrete structure. The major contributions behind our work are as follows:

- An experimental study are made on the identification of corrosion mechanism in different types of reinforced concrete containing class – *F*Fly ash and steel bar with different fine aggregates such as river sand and manufactured sand.
- Analyzes is done in different curing conditions to find out corrosion attack on fly ash concrete structure.
- Investigation is carried out the corrosion process in embedded steel bar by using Tafel polarization and AC Impedance methods by using ACM Instruments (UK).
- Inference from the study is carried out such as Tafel polarization and AC Impedance the test results obtained shows 1% to 2%variations.

The rest of this work is summarized as follows: Section 2 demonstrates the materials and methods used in this experimental study. Section 3 describes the methodology of corrosion steel mechanism. Section 4 exhibits the experimental

CONTACT J. Mahesh jmaheshcivil@gmail.com Udhya School of Engineering, Tamil nadu, India
Present affiliation for T. Jarin is Department of Electrical Engineering, APJ Abdul Kalam Technological University, Trichur, Kerala

study of Tafel polarization and AC Impedance methods. Finally, this work ends up with conclusion in section 6.

2. Materials and methods

2.1. *Materials*

Concrete of M45 grade with mix designed DOE method, OPC-43 Grade cement (DALMIA) conforming to IS:8112:1989, River sand washed conforming to Zone-III (Trichy), Manufactured sand available at local quarry (Chitramcode), Coarse aggregate 20m mangular granite stones conforming to IS:383:1970 (Chitramcode), Fly ash-F from Thoothukudi thermal power plant conforming to IS:3812PART-I-2003, Teflon coated copper wire and portable water. The reinforcement used Fe500 grade 16mm diameter steel bar (TATA Tiscon) [10].

2.2. *Specimen preparations*

In order to perform the Totally 12 numbers of samples were cast. Every pair is designated as $F_{20R,}$ $F_{20M,}$ $F_{30R,}$ $F_{30M,}$ F40R, and F40M. Numbers 20, 30, 40 indicate percentage of fly ash, *M*and *R*indicate the fine aggregates (Manufactured sand and River sand). The size of cube mould is 15 cm×15 cm × 15 cm.The tamping rod 75mm long and 16mm diameter is for compaction. The concrete mix design is by DOE method and $\frac{W}{C}$ratio is calculated as per mix design. The materials are measured by weigh batching. The cube mould is cleaned by mould releasing agent. Then the cube is filled in three equal layers, each layer with the height of 5cm.The concrete mixture is placed up to first layer subject to compaction by using tamping rod 35 times strokes applied. Again concrete placed up to second layer subject to compaction by using tamping rod 35 times strokes applied. Subsequently concrete is filled up to top of cube mould subject to compaction by using tamping rod 35 times strokes applied.

Finally the concrete is struck off at top level by using trowel. The 16mm diameter 10cm length reinforcement with Teflon coated copper wire bound and sealed by M-seal embedded vertically in the centre of the cube. The clear cover of 25mm top and bottom, 67mm is used in all four sides. The specimens are stored in the place free from vibration and moist air of at least 90%relative humidity and temperature of $27^{\circ}c \pm 2^{\circ}c$.After 24 hours of initial setting the specimens are removed from the mould [11]. Six numbers of specimens are submerged in clean fresh water tank for curing. Six numbers of specimens are transported by vehicles to Arabian Sea in Colachal Sea shore in Kanyakumari District, Tamil Nadu, India and submerged in sea water in covered fishnet. Fishnet is bound near rock by nylon rope. After 180 days of curing, the test specimens are taken out from curing tank and sea water and transported to concrete corrosion department research lab CSIR-CECKRI Karaikudi, Where the corrosion analysis is done by using ACM Instrument. The samples were cast on 19/08/2015, tested on 15/02/2016 with the test period of 181 days. Table 1 shows the mix design result of DOE method.

3. Methodology

3.1. *Corrosion mechanism of steel*

Corrosion of reinforcement is complex procedure. It is an electrochemical process similar to that of a simple battery. When there is a difference in electrical potential along the steel reinforcement in concrete, an electro chemical cell is set up in the reinforcement as explained by [12,13]. One part of steel becomes anode (more negatively charged) and other part of steel becomes cathode (positively charged). Concrete is capable of conducting current act as electrolyte with the circuit being completed by the reinforcement through the electron can flow [14]. The positively charged ferrous ions Fe^{++}released from a node combine with the hydroxyl ions (OH^{-}) from the cathode in the presence of water and oxygen. Then they travel through the electrolyte and combine with the ferrous ions to form ferric hydroxide$Fe(OH)$) which is converted by further oxidation to rust. The rust occupies a volume as many as six times of the original volume of steel depending upon the oxidation state. This is an expansive reaction. The increased volume of rust exerts thrust leading to cracks, spalling or delaminating of concrete on cover. In these kinds of situations concrete loses its integrity [15]. The cross sectional area of reinforcement progressively reduces and the structure is sure to collapse. The reactions are described below: Figures (1 and 2) depicts mechanism of steel corrosion and oxidation state of iron.

Anodic reactions:

$$Fe \rightarrow Fe^{++} + 2e \tag{1}$$

$$Fe^{++} + 2(OH^{-}) \rightarrow Fe(OH)_2 \,(\text{Ferrousoxide}) \tag{2}$$

$$4Fe(OH)_2 + 2H_2O + O_2 \rightarrow 4Fe_2O_3 \,(\text{Ferricoxide}) \tag{3}$$

Cathodic reactions:

$$4e^{-} + O_2 + H_2O \rightarrow 4(OH^{-}) \tag{4}$$

Hydration process of fly ash with cement and pozzolonic reaction:

$$OPC + Water = C - S - H_{(durable\ \ binder)} + CA(OH)_{2(non-durable\ \ binder)} \tag{5}$$

$$OPC + H_2O = C - S - H_{gel} + CA(OH)_2 \tag{6}$$

Table 1. Mix design result (DOE method).

Sl.no	sample	Fly Ash (%)	Cement Kg/M^3	Fly ash Kg/M^3	F.A Kg/M^3	C.A Kg/M^3	Water Kg/M^3	W/C Ratio	Mix Ratio
1	F_{20R}&F_{20M}	20	391.67	97.91	629.25	1071.43	199.74	0.407	1:1.28:2.18
2	F_{30R}&F_{30M}	30	354.47	151.97	604.48	1074.64	189.89	0.375	1:1.19:2.12
3	F_{40R}&F_{40M}	40	324.56	216.37	633.40	1056.40	184.99	0.342	1:1.17:2.08

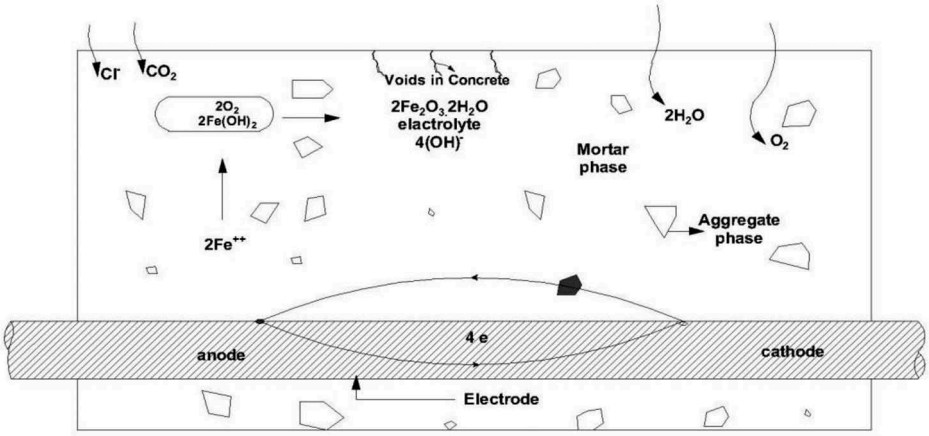

Figure 1. Diagrammatical representation of corrosion mechanism of steel.

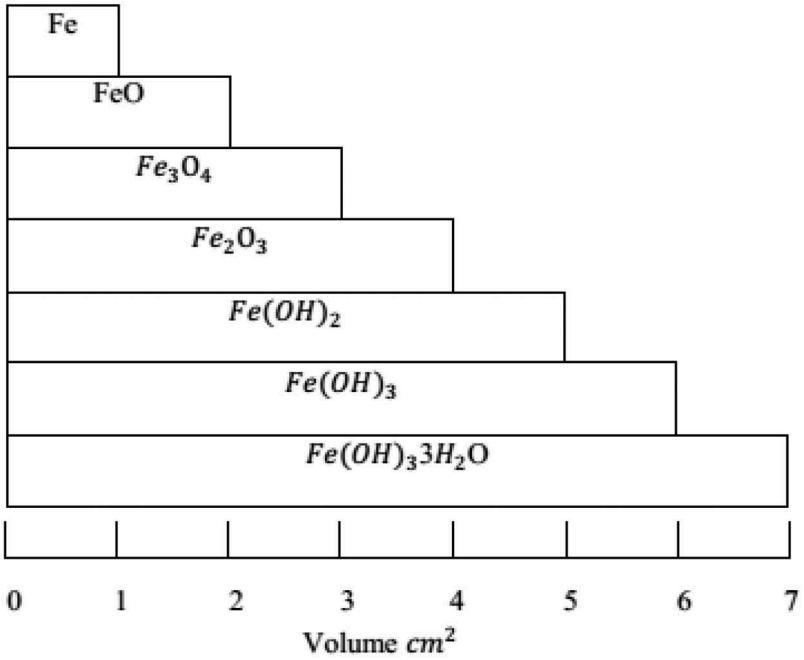

Figure 2. Oxidation state of iron in volume.

$$OPC + H_2O + Fly\ ash = C - S - H_{(durable\ binder)} + CA(OH)_{2(non-durable\ binder)} + fly\ ash \quad (7)$$

$$CA(OH)_2 + fly\ ash = C - S - H_{gel} \quad (8)$$

4. Experimental study

4.1. *Tafel polarization studies*

Polarization methods are faster and gives better experimental results . Three electrode cells are used for measurement of polarization resistance in a laboratory. They are (i) Working electrode (Rebar), (ii) Counter electrode (Stainless steel 316L), (iii) Reference electrode ('Calomel'Hg_2Cl_2).Tafel relationship with respect to under activation control in the electrochemical process linear polarization curves exhibits $EV_s \log(i)$ plots called Tafel behavior. After the electro injection process, the same set-up was made use of for polarization measurements to evaluate the corrosion kinetic parameters such as corrosion potential(E_{corr}), anodic Tafel slope(ΔE), corrosion-current(I_{corr}), and cathodic Tafel slope(Δ_i). Both cathodic and anodic polarization curves were recorded potentio-dynamically using Gill AC (500 mA/100 kHz/Guard ring of *ACM* Instruments UK [14]. These instruments have inbuilt software support to evaluate corrosion kinetic parameters in digital and graphical form and tested in CEKRI lab (Figure 3). The potentio-dynamic conditions correspond to a potential sweep rate of 6 mvmin^{-1}and starting potential −200 mV final potential 200 mV from the *OCP*. All the experiments were carried out at constant temperature of 32 ± 1°C.

$$I_{corr} = \beta_a\beta_c/2.3Rp(\beta_a + \beta_c) \quad (9)$$

Whereas, $\beta_a\beta_C$=Tafel Constant (Figure 4) calculated from anodic and cathodic slope Corrosion rate

$$(mb) = 0.13_{corr} \times E.\frac{W}{dA} \quad (10)$$

Hence, $E.W$ =equivalent weight of steel (g) and $d =$ density of reinforcing steel (g/cm^3)

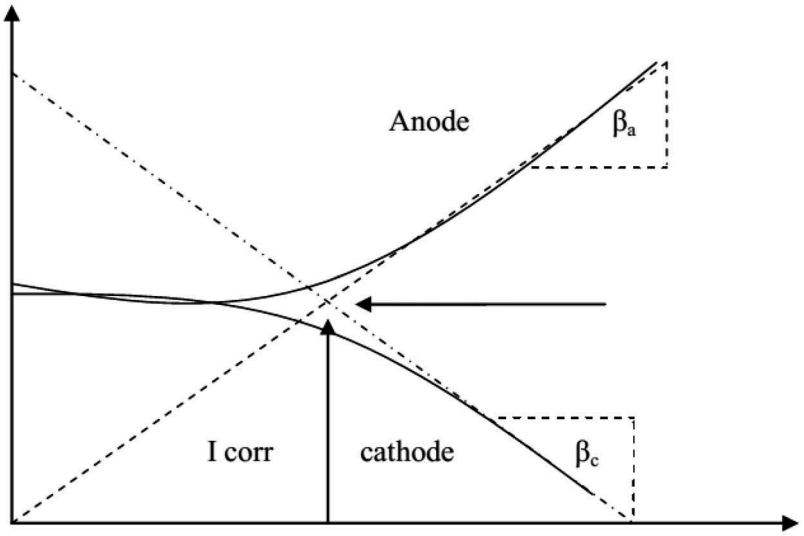

Figure 3. Testing in CEKRI lab.

Figure 4. Tafel plot to estimate Tafel constants.

$$R_p = \Delta E/\Delta_i(\Delta E \to 0)k\Omega cm^2 \quad (11)$$

The term $R_P$is defined as Polarization resistance

4.1.1. *Experimental report*

As per curing condition by using:

(1) River Sand
(2) Manufactured sand
(3) 20%, 30%, 40% fly ash replacement samples subject to sea water curing corrosion rates are 6.399, 4.611, 3.577 have more corrosion rate than ordinary water curing the corrosion rates are 5.301, 3.350, 3.422 (Figure (7(a,b)) and Table 2).
(4) 20%, 30%, 40% fly ash replacement samples subject to sea water curing the corrosion rates are 6.408, 4.699, 5.724 have more corrosion rate than ordinary water curing the corrosion rates are 5.488, 3.371, 4.625 (Figure (7(c,d)) and Table 2)

As per fine aggregate used in the different exposure condition:

(1) Sea environment
(2) Atmospheric environment
(3) Corrosion rate of 20%, 30%, 40% fly ash replacement samples by using river sands are 6.399, 4.611, 3.577 have lesser corrosion rate than manufactured sands the corrosion rates are 6.408, 4.699, 5.724 (Refer:- Figure (7(a,c)) and Table 2).
(4) Corrosion rate of 20%, 30%, 40% fly ash replacement samples by using river sands are 5.301, 3.350, 3.422 have lesser corrosion rate than manufactured sands the corrosion rates are 5.488,3.371,4.62 (Refer:- Figure (7(b,d)) and Table 2). As per % of fly ash replacement.
(5) Corrosion rate is 20%> 40% > 30%. 30% fly ash replacement samples show Less corrosion rate than 40% and 20% in all exposure condition (Refer:- Figure (7(a–d)) and Table 2).

4.1.2. *Analysis*

4.1.2.1. ***ACM instruments (UK) produced tafel polarization graphs.*** Impedance graph generated for river sand with two types of curing like sea water curing and ordinary water curing. Figure 5 (c, d): Impedance graph generated for manufactured sand with sea water curing and ordinary

Table 2. Tafel polarization test result.

System	curing type	FA	OCP mV	E_{corr} mV	ΔE $mV.dec^{-1}$	Δi $mV.dec^{-1}$	$I_{corr}\times 10^{-5} mA.cm^{-2}$	C_{orr}rate$\times 10^{-4}$mpy
F_{20M}	Sea water	M sand	−329	−388	90	72	5.529	6.408
	water	M sand	−147	−231	114	68	4.390	5.488
F_{20R}	Sea water	R sand	−450	−484	76	67	6.523	6.399
	water	R sand	−214	−295	109	67	4.457	5.301
F_{30M}	Sea water	M sand	−327	−380	96	66	4.050	4.699
	water	M sand	−228	−298	78	57	2.909	3.371
F_{30R}	Sea water	R sand	−349	−404	111	73	4.583	4.611
	water	R sand	−147	−221	105	57	2.877	3.350
F_{40M}	Sea water	M sand	−763	−773	82	76	4.938	5.724
	water	M sand	−463	−503	97	76	3.990	4.625
F_{40R}	Sea water	R sand	−249	−337	112	67	3.292	3.577
	water	R sand	−214	−286	100	68	2.953	3.422

Figure 5. Complex impedance graphs generated with mixing (Figure 6) and Figure 7 weighing& casting the sample (a, b).

water curing In the following graph, Figure (7(a)) illustrates the change of potential E_{corr}(mV) with corrosion current I_{corr} (mA/cm^2) of 20%, 30%, 40% fly ash replacement concrete sample using river sand as fine aggregate and sea water curing. Figure (7(b)) illustrates the change of potential E_{corr} (mV) with corrosion current I_{corr} (mA/cm^2) of 20%, 30%, 40% fly ash replacement concrete sample using river sand as fine aggregate and ordinary water curing. From Tafel curve we can find out anodic slope and cathodic slope ΔE and Δ_i. In the following graph, Figure (7(c)) illustrates the change of potential E_{corr}(mV) with corrosion current I_{corr}(mA/cm^2) of 20%, 30%, 40% fly ash replacement concrete sample using manufactured sand as fine aggregate and sea water curing. Figure (7(d)) illustrates the change of potential E_{corr}(mV) with corrosion current I_{corr} (mA/cm^2) of 20%, 30%, 40% fly ash replacement concrete sample using manufactured sand as fine aggregate and ordinary water curing. From Tafel curve we can find out anodic slope and cathodic slope ΔE andΔ_i

4.2. *AC impedance method*

Impedance is the frequency domain ratio of complex voltage to the current amplitude. Complex voltage V_0 and current amplitude I_0 thus obeys the linear relation $\hat{V} = \hat{I}Z$. which is complex generalization of ohm's law$V = IR$. The impedance of a resistor is just the resistance, which can be calculated by complex division of the voltage and current after the electro injection process TMT steel rebar embedded in concrete specimens were subjected to AC impedance measurements. The same three electrode cell assemblies were used here also. The real part (Z') and the imaginary part $(-Z'')$of the cell impedance were recorded for various frequencies ranges of (30,000–0.01 Hz) [17]. Plots of $-Z'$in X-axis versus $-Z''$in Y-axis were made. The complex impedance graph illustrated in Figure (7) and 8 is for various mixes of Figures 6 and 6. Polarization $R_P$data obtained from the DC technique based on the previous study, the corrosion current density can be computed from the following equation.

$$I_{corr} = \beta_a\beta_c/2.30Rp(\beta_a\beta_c) \tag{12}$$

Whereas, β_a = Anodic Slope,β_c = Cathodic Slope,R_p = Polarization Resistance

$$\text{Corrosionrate(mm/yr)}=0.129\ I_{corr} \times \frac{E.W}{d_a} \tag{13}$$

$$\text{Impedance } Z = |Z|e^{i\theta} \tag{14}$$

i = Imaginary unit, θ =Phase difference between voltage and current

$$e^{i\theta} = \frac{V_0}{I_0} \tag{15}$$

V_0 = complex voltage, I_0 = complex current

$$|Z| = \frac{V_0}{I_0} \tag{16}$$

V_0 = Real amplitude of voltage, I_0 = Real amplitude of current

4.2.1. *Experimental report*

Figure 9, 10, 11 and 12 shows the CEKRI lab and Electrode sample with detail experimental setup.

As per curing condition by using:

(1) River sand
(2) Manufactured sand
(3) 20%,30%,40% fly ash replacement samples subject to sea water curing 9.523,6.935,5.160 have more corrosion rate than ordinary water curing 7.149,3.656,2.967 (Refer:-Figure (13 (a,b)) and Table 3).
(4) 20%, 30%, 40% fly ash replacement samples subject to sea water curing 9.988, 7.214, 5.415 have more corrosion rate than ordinary water curing 7.209, 3.710,3.570 (Refer:- Figure (13(c,d)) and Table 3).

As per Fine aggregate used in the different exposure condition:

(1) Sea Environment
(2) Atmospheric Environment

Figure 6. Mixing.

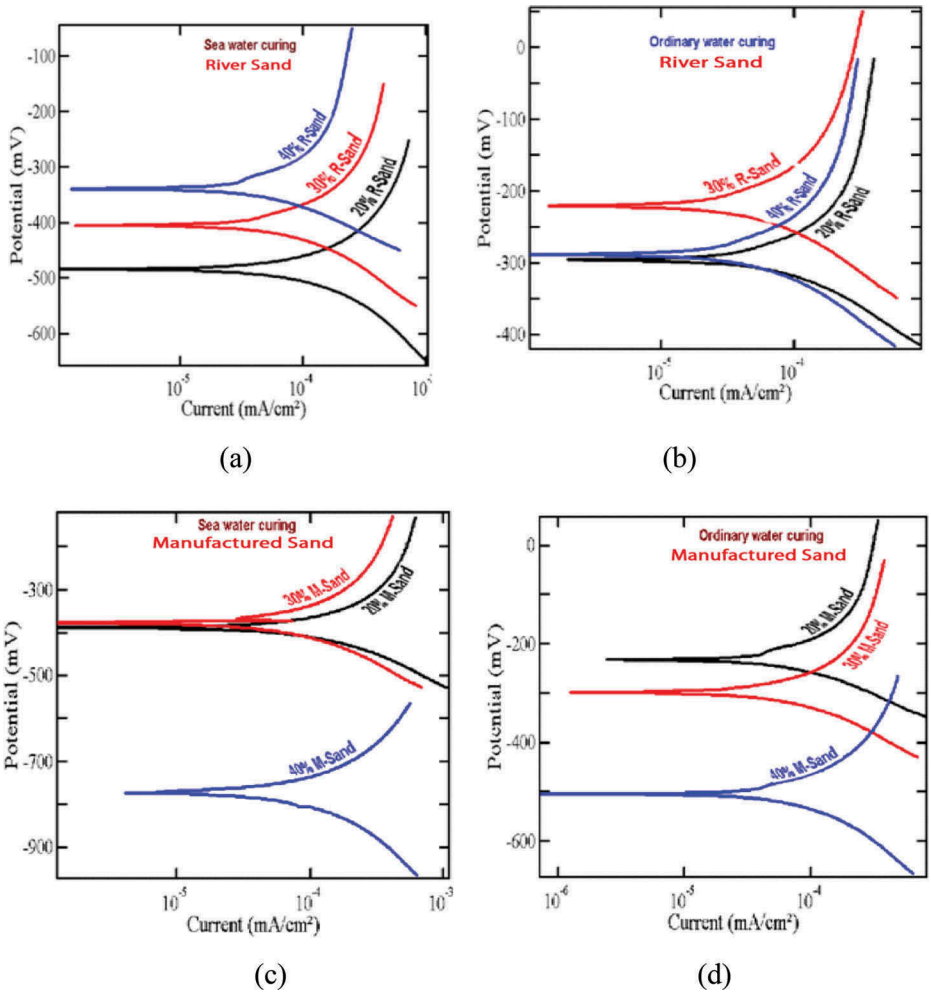

Figure 7. Weighing & casting the sample.

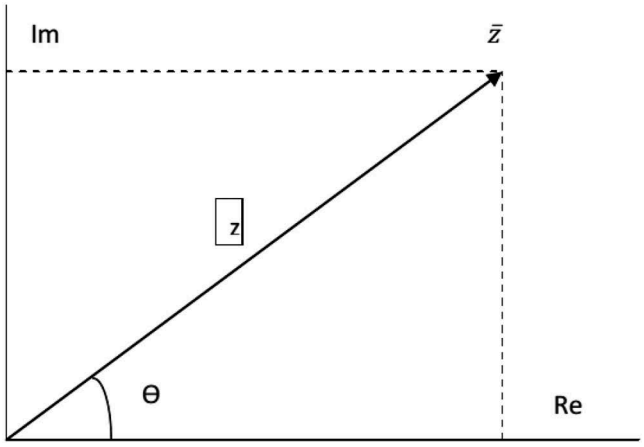

Figure 8. Test CEKRI lab.

(3) 20%, 30%, 40% fly ash replacement samples by river sand 9.523, 6.935, 5.160 have more corrosion rate than manufactured sand 9.988, 7.214, 5.415 samples (Refer:- Figure (13(a,b)) and Table 3).
(4) 20%, 30%, 40% fly ash replacement samples by river sand 7.149, 3.656, 2.967 have lesser corrosion rate than manufactured sand 7.209, 3.710, 3.570 samples (Refer: Figure (13 (b,d)) and Table 3).

As per % of fly ash replacement:

(1) Corrosion rate is 20% > 40% > 30%. 30% fly ash replacement samples show lesser corrosion rate than 40% and 20% (Refer:-Figure (13 (a–d)) and Table 3).

4.2.2. *Analysis*

4.2.2.1. *ACM instruments (UK) produced AC impedance graphs.* In the following graph, Figure(13(a)) illustrates the real part $R(Z')$Versus imaginary part $Im(Z'')$of 20%,30%,40% fly ash replacement concrete sample using river sand as fine aggregate and sea water curing. Figure (13(b)) illustrates the real part $R(Z')$Versus imaginary part $Im(Z'')$of 20%,30%,40% fly ash replacement concrete sample using river sand as fine aggregate and ordinary water curing. In the following graph, Figure (13(c)) illustrates the real part $R(Z')$Versus imaginary part $Im(Z'')$of 20%, 30%, 40% fly ash replacement concrete sample using manufactured sand as fine aggregate and sea water curing . Figure (13(d)) illustrates the real part $R(Z')$Versus imaginary part $Im(Z'')$of 20%, 30%, 40% fly ash replacement concrete sample using manufactured sand as fine aggregate and ordinary water curing .

5. Conclusion

In our studies and experiments, as per test result had shown, 20%, 30% and 40% fly ash replacement reinforced concrete samples with replacement of fine aggregate by manufactured sand concrete samples. The steel reinforcement corroded faster than river sand used concrete samples. Also it is subjected

Table 3. AC impedance test result.

System	curing type	FA	Rs× 10^5 ($\Omega.cm^2$)	Rct× 10^4 ($\Omega.cm^2$)	Cdl× 10^{-5} ($F.cm^{-2}$)	I_{corr}× 10^{-4} ($mA.cm^{-2}$)	C_{orr}rate× 10^{-3} (mpy)
F_{20M}	Sea water	M sand	1.291	3.027	1.868	8.618	9.988
	Water	M sand	1.820	4.194	1.076	6.220	7.209
F_{20R}	Sea water	R sand	1.494	3.175	1.736	8.216	9.523
	Water	R sand	1.770	4.229	2.533	6.169	7.149
F_{30M}	Sea water	M sand	2.087	4.191	0.511	6.225	7.214
	Water	M sand	2.316	8.149	5.802	3.201	3.710
F_{30R}	Sea water	R sand	1.710	4.360	1.132	5.983	6.935
	Water	R sand	2.335	9.702	0.622	2.689	3.656
F_{40M}	Sea water	M sand	3.862	6.848	0.126	3.809	5.415
	Water	M sand	2.417	8.470	0.9370	3.086	3.570
F_{40R}	Sea water	R sand	2.147	5.860	0.251	4.452	5.160
	Water	R sand	4.957	10.190	1.638	2.560	2.967

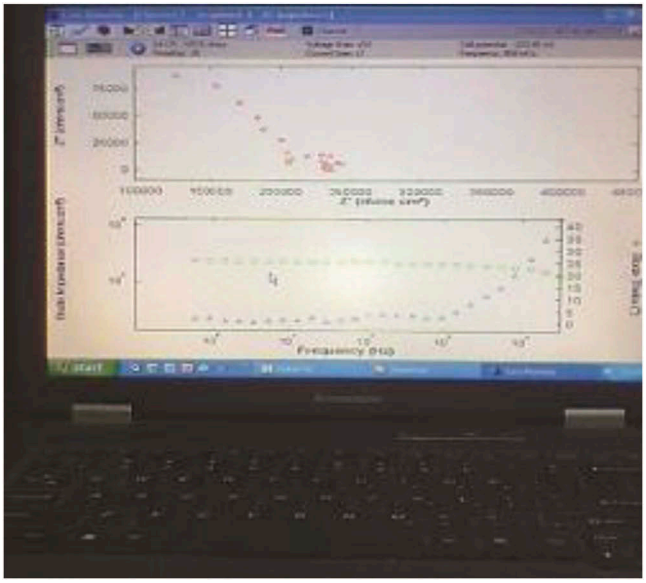

Figure 9. Curing at Colachal Arabian Sea.

Figure 10. AC impedance graphs generated with Figures 8 and 10. Figure 13 (a, b): impedance graph generated for river sand with sea water curing and ordinary water curing. Figure 13 (c, d): impedance graph generated for manufactured sand with sea water curing and ordinary water curing.

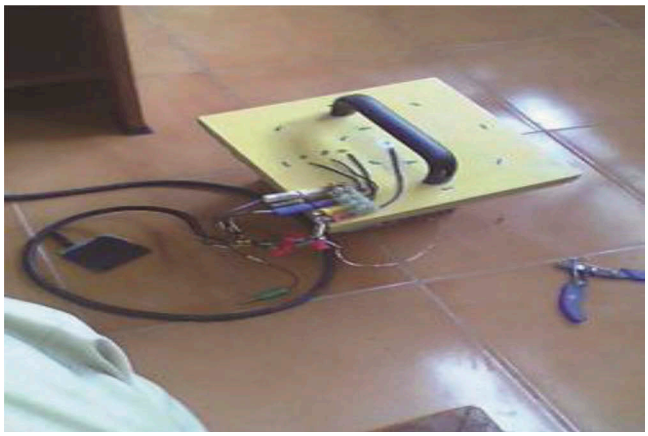

Figure 11. AC impedance graphs generated with Figures 8 and 10. Figure 13 (a, b): impedance graph generated for river sand with sea water curing and ordinary water curing. Figure 13 (c, d): impedance graph generated for manufactured sand with sea water curing and ordinary water curing.

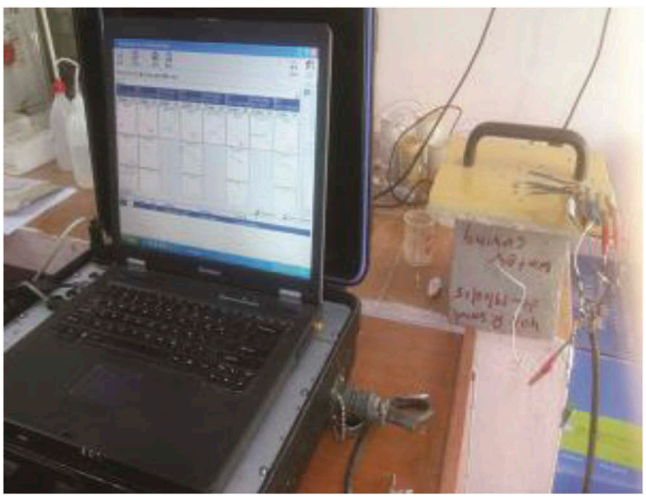

Figure 12. AC impedance graphs generated with Figures 8 and 10. Figure 13 (a, b): impedance graph generated for river sand with sea water curing and ordinary water curing. Figure 13 (c, d): impedance graph generated for manufactured sand with sea water curing and ordinary water curing.

to different curing condition such as sea water and portable water. The steel reinforcement in the concrete sample subject to sea water curing corroded faster than portable water curing and also in the basis of percentage of fly ash used in different curing condition and fine aggregate replacement 20% fly ash replacement concrete samples corroded faster than 30% and 40% fly ash replacement reinforced concrete. But 30% fly ash replacement reinforced concrete samples subject to above curing condition and replacement of fine aggregates, the steel reinforcement corroded slower than 40% fly ash replacement reinforced concrete samples. Hence the study positively advocates for 30% fly ash replacement with river sand as fine aggregate subject to potable water curing. Also, manufactured sand is good as fine aggregate replacement for 30% fly ash replacement reinforced concrete. The variation

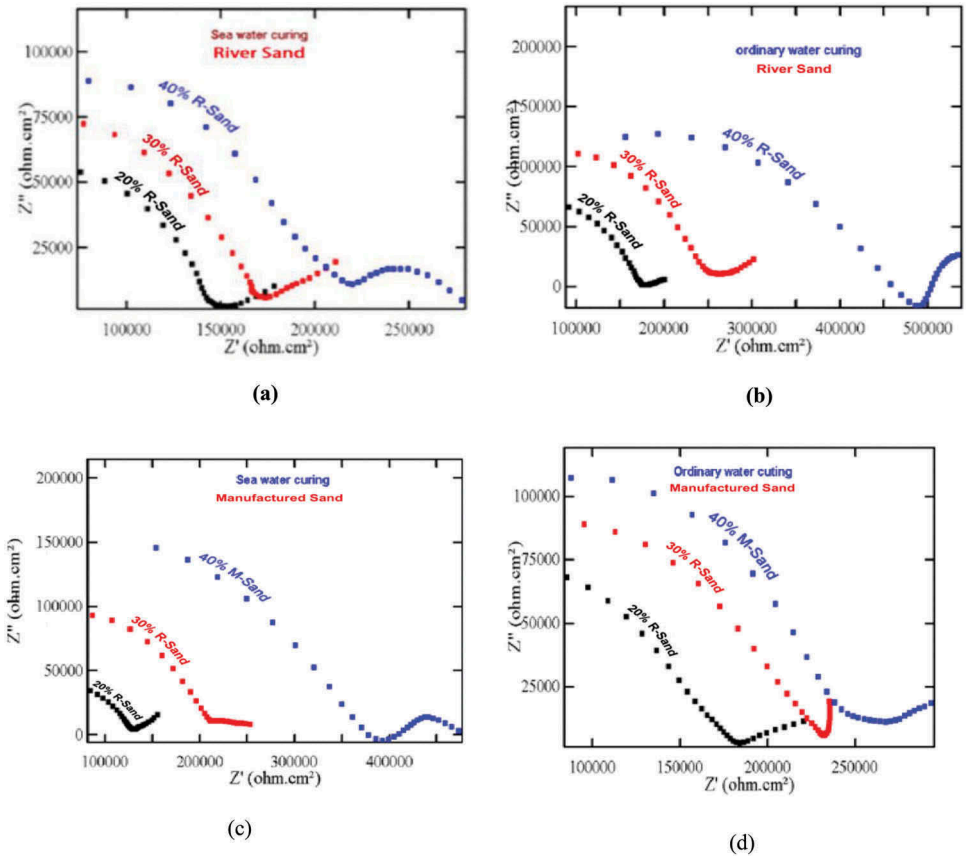

Figure 13. AC impedance graphs generated with Figures 8 and 10. Figure 13 (a, b): impedance graph generated for river sand with sea water curing and ordinary water curing. Figure 13 (c, d): impedance graph generated for manufactured sand with sea water curing and ordinary water curing.

shows in the test results only 1.9% in sea water curing and 0.62% in potable water curing between river sand and manufactured sand test samples. In the above two experiments Tafel polarization and AC Impedance the test results shown 1% to 2% variations.

Acknowledgments

The laboratory used for sample preparation concrete is highway laboratory located in Udaya School of Engineering. The laboratory used for conducting tests in concrete corrosion isone of the famous lab in the department research laboratory CSIR-CECKRI Karaikudi. I would like to thank Dr.Muralidhran senior scientist concrete corrosion department CEKRI Karaikudi for helped me to do experiments in CEKRI laboratory. I would also like to thank students of final year 2015 batch Udaya school of Engineering to assist me to prepare the test samples.

Disclosure statement

No potential conflict of interest was reported by the authors.

Notes on contributors

J. Mahesh He received his B.E and M.E degrees in Civil Engineering from Anna University. He is pursuing his PhD in Anna University in the faculty of civil engineering. He is working as Assistant Professor in Udhya School of Engineering. His research interests are concrete structures.

K. Nagamani He completed his B.E(Hons.) Civil Engineering at PSG College of Technology of University of Madras. He has completed his M.Tech with Distinction in Ocean Engineering and Ph.D in Offshore Structures at I.I.T. Madras. He is currently Professor and Head of Department of Civil Engineering in Anna University, Guindy campus Chennai.His areas of interests are Earthquake Design,Structural Dynamics,and Offshore Structures.

Dr. T. Jarin He received his B.E, M.E,and Ph.D degrees in Electrical Engineering from Anna University. He is working as Associate Professor and Head of Department/EEEin Jyothi engineering college of Kerala. His research interests are Automation in Buildings, Electric Resistivity in Materials, Nano CoatingandPower Drives.

References

[1] Harandi SE, Banerjee PC, Christopher DE, et al. Influence of bovine serum albumin in Hanks' solution on the corrosion and stress corrosion cracking of a magnesium alloy. Mater Sci Engineering: C. 2017 Nov 1;80:335–345.
[2] Kumar V, Singh R, Quraishi MA. A study on corrosion of reinforcement in concrete and effect of inhibitor on service life of RCC. J Mater Environ Sci. 2013;4.5:726–731.
[3] Noeiaghaei T, Mukherjee A, Dhami N, et al. Biogenic deterioration of concrete and its mitigation technologies. Constr Build Mater. 2017 Sep 15;149:575–586.
[4] Shanmugam S, Srisanthi VG, Ramachandran S. Effects of corrosion on reinforced concrete beams with silica fume and polypropylene fibre. Proceedings of World Academy of Science, Engineering and Technology. No. 74. World Academy of Science, Engineering and Technology (WASET); 2013.
[5] Polder RB. Effects of slag and fly ash on reinforcement corrosion in concrete in chloride environment: research from the Netherlands. Heron. 2012;57:3.
[6] Marcos-Meson V, Michel A, Solgaard A, et al. Corrosion resistance of steel fibre reinforced concrete - A literature review. Cem Concr Res. 2018 Jan;103:1–20.
[7] Kumar MK, Rao PS, Swamy BLP, et al. Corrosion resistance performance of fly ash blended cement concretes. Int J Res Eng Technol. 2012;1(3):448–454.
[8] Llau A, Jason L, Dufour F, et al. Finite element modelling of 1D steel components in reinforced and prestressed concrete structures. Eng Structures. 2016 Nov 15;127:769–783.

[9] Fu X, Chung DDL. Effect of corrosion on the bond between concrete and steel rebar. Cem Concr Res. 1997 Dec;27 (12):1811–1815.
[10] Jiang D, Tan KH, Wang CM, et al. Analysis and design of floating prestressed concrete structures in shallow waters. Marine Structures. 2018 May;59:301–320.
[11] Sounthararajan VM, Sivakumar A. Corrosion measurements in reinforced fly ash concrete containing steel fibres using strain gauge technique. Int J Corrosion. 2013;2013: 7. Article ID 724194.
[12] Song H-W, Saraswathy V. Corrosion monitoring of reinforced concrete structures-A. Int J Electrochem Sci. 2007;2:1–28.
[13] Barnes CL, Trottier J-F, Forgeron D. Improved concrete bridge deck evaluation using GPR by accounting for signal depth-amplitude effects. NDT & E Int. 2008 Sep;41(6):427–433.
[14] Huang R, Yeih WD, Chang JJ, et al. The use of ac and dc methods for corrosion monitoring of reinforced concrete members in marine environment. J Marine Sci Technol. 1999;2 (1):53–59.
[15] Saraswathy V, Muralidharan S, Thangavel K, et al. Influence of activated fly ash on corrosion-resistance and strength of concrete. Cem Concr Compos. 2003;25(7):673–680.